

CARDIAC CYCLE ARTEFACT REMOVAL IN MAGNETOENCEPHALOGRAPHIC DATA OF PATIENTS WITH DEEP BRAIN ELECTRODES

Implementation of Simultaneous Magnetoencephalographic and Local Field Potential Recordings

Antje Bock¹, Andrea A. Kühn¹, Lutz Trahms² and Tilmann H. Sander²

¹Department of Neurology, Charité Berlin, Campus Virchow, Augustenburger Platz 1, 13353 Berlin, Germany

²Physikalisch-Technische Bundesanstalt, Abbestr. 2-12, 10587 Berlin, Germany

Keywords: Magnetoencephalography, Deep brain stimulation, Local field potentials, Cardiac cycle artefact, Principal component analysis, Signal space projection, Coherence.

Abstract: Simultaneous magnetoencephalography (MEG) and local field potential (LFP) recordings in patients undergoing deep brain stimulation (DBS) for severe movement disorders is a promising technique both for clinical applications and basic research. Recordings can be accomplished during the time interval between electrode insertion and implantation of the stimulator while electrodes are externalised. At present, strong cardiac cycle artefacts (CCA) are observed in the MEG signals around the area, where the disposable stainless steel electrode wires leave the skull. The CCA refers to the remanent magnetic field of those wires underneath the sensors, which are moved by local pulsations of the blood vessels. Here, we demonstrate a new approach to partially remove the CCA by applying principal component analysis (PCA) to an averaged CCA and subsequent signal space projection (SSP) method. Further steps of analysis such as coherence calculations are less distorted after SSP.

1 INTRODUCTION

Deep brain stimulation (DBS) offers the unique opportunity to directly record local field potentials (LFP) from the human basal ganglia (BG) (Silberstein et al., 2003; Kühn et al., 2004). By implementing simultaneous magnetoencephalography (MEG) and LFP recordings in patients undergoing DBS, cortical brain activity in terms of magnetic fields in addition to electrical neuronal activity directly from the BG can be measured. Results will give fundamentally new insights about information encoding and processing in the cortico-BG network. However, MEG recordings are very noisy due to the cardiac cycle artefact (CCA). The CCA refers to local pulsations of the blood vessels moving the weakly magnetised (externalisation) stainless steel electrode wires relative to the MEG sensors (Litvak et al., 2010). The principal component analysis (PCA) of the averaged CCA can be calculated in order to identify the pattern and dimensionality of the artefact, which, in turn, can then be eliminated from the MEG data by applying signal

space projection (SSP). Subsequent coherence calculations lead to improved topographic distributions.

2 METHODS

2.1 Patients and Recordings

Nine patients with Parkinson's disease (PD) (2 females, mean age 55.89 ± 11.53 years) and eight patients suffering from dystonia (5 females, mean age 51.50 ± 8.38 years) were included in this study (17 in total). DBS electrodes were implanted bilaterally in the subthalamic nucleus (STN) in the PD patients or in the internal globus pallidus (GPi) in the dystonic patients, respectively. During the time interval (2 to 5 days) before connection of the electrodes to a subcutaneous pulse generator, simultaneous LFP and MEG recordings can be accomplished. To this end, patient's heads were positioned in a 125-channel whole head MEG system (KIT, Eagle Technology, Kanazawa, Japan). Rest recordings of 300 s

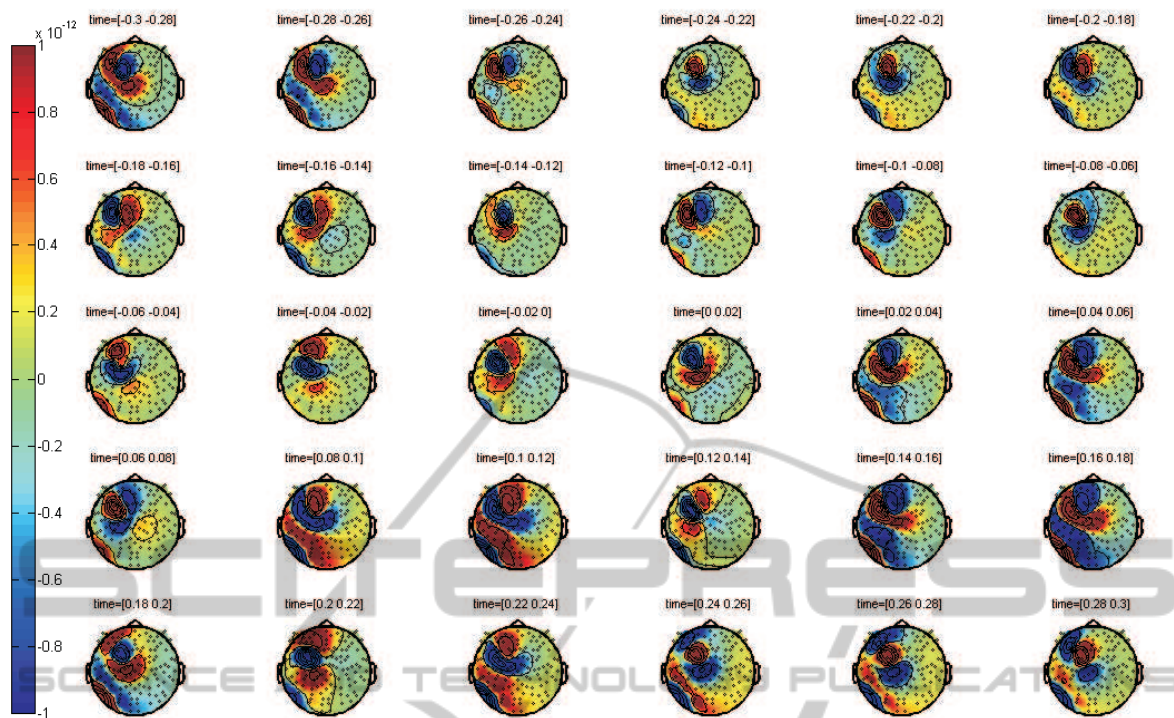


Figure 1: Averaged CCA of a dystonic patient calculated by R peak alignment (field strength indicated in Tesla).

duration were made while patients were asked not to move and keep their eyes open. Simultaneously with changes of the magnetic flux, LFP signals were acquired with a 32 channel low noise EEG amplifier. The DBS macroelectrodes in each hemisphere comprise 4 contacts, which are numbered 0, 1, 2, and 3 with 0 being the most caudal one. LFP signals were recorded using contact 0 of the left electrode as a common reference and then re-referenced to bipolar signals by subtracting adjacent contact pairs from each other. Additionally, electrocardiograms (ECGs) were recorded monopolarly with reference to the left deep brain electrode contact 0. A ground electrode was placed on the patient's forehead. Data were sampled at 2000 Hz and off-line filtered between 5 and 120 Hz. PD patients were recorded twice in one session, once after overnight withdrawal from dopaminergic medication (OFF) and 30 to 60 minutes after intake of 200 mg of L-DOPA (ON).

2.2 Cardiac Cycle Artefact Removal

In MEG data, the heartbeat generates the cardiac artefact (CA). The CA reflects the electrical current within the heart muscle (Jousmäki and Hari, 1996), which is a significant contribution to the MEG even though MEG is recorded at a distance of about 200 mm from the heart. In patients with externalised elec-

trode wires, a second artefact can be detected, which is the cardiac cycle artefact (CCA) (Litvak et al., 2010). The CCA refers to the time variable magnetic field due to local pulsations of the blood vessels moving the weakly magnetised externalisation wires relative to the MEG sensors. Both artefacts are best identified by finding the R wave, which is the deflection of highest amplitude within the electrocardiographic QRS complex. The QRS complex reflects the depolarisation of the heart's right and left ventricles and lasts about 100 ms. The CCA is of much higher amplitude than the CA as it has a technical origin, for which reason the CA can be ignored within the scope of this work. The R peak of the ECG signal has then been used as a trigger for averaging the CCA in all channels with trials of 600 ms length (300 ms before and 300 ms after trigger onset).

As it can be assumed that the magnetic and electric fields propagate instantaneously, the averaged CCA (aCCA) can be calculated by time-locking the magnetic channels to the ECG. Figure 1 shows the resulting topographic maps of all magnetic channels (the number of the remaining channels of each patient varied between 90 and 110, because saturated channels close to the artefact source have been sorted out) for time epochs of 20 ms. The patient's head in the map is seen from above with sketched ears and nose to denote its orientation. The little black dots indicate

the locations of the sensors. The aCCA is the pattern that is located within the left hemisphere around the fronto-parietal area, where the electrode wires are placed in loops underneath the skin. The intensity of the magnetic field changes are color-coded and given in Tesla. Positive values are shown in yellow, orange and red color shades and represent sources, while negative blue-colored values show sinks. Arterial blood flow velocity is about 1 m/s in thick blood vessels, therefore the temporal allocation of the aCCA pattern differs from the one of the QRS complex and the strongest aCCA signal appears later than the R peak at 0 ms.

A common method to detect the dimensionality of a multivariate data set is the PCA. PCA using the covariance method is an orthogonal linear transformation into uncorrelated variables (principal components) by calculating the eigenvalue decomposition of a covariance matrix. The PCA of the CCA can now be calculated in order to identify the pattern and dimensionality of the artefact. Figure 2 shows all patients' ($m = 26$) resulting set of the first 30 eigenvalues in decreasing order. The eigenvalues represent the energy of the eigenvectors. Eigenvalues have been standardised to the maximum eigenvalue being 1, as the magnetisation of the electrode wires differs among patients. A sharp bend at the fifth eigenvalue can be seen in all curves, indicating that the dimensionality of the CCA is $5 \leq dim_{CCA} \leq 10$ and fairly similar for all data sets.

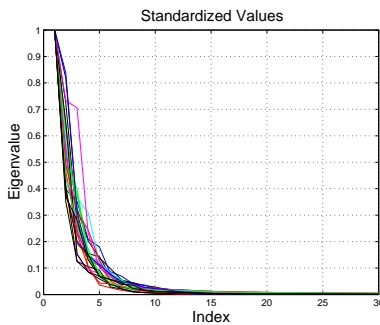


Figure 2: First 30 standardised eigenvalues ($m = 26$) of the PCA.

Given that the PCA eigenvalues of the aCCA have a similar dependence, it is reasonable to use the signal space projection (SSP) method as proposed by Uusitalo and Ilmoniemi (Uusitalo and Ilmoniemi, 1997) to suppress the most powerful CCA components from the data set. For this, the PCA decomposition is backprojected to the channel level after removing the first five principal components. If $A_{1,\dots,n}$ ($90 \leq n \leq 110$) is the matrix containing the sorted eigenvectors $eigenvector_1, eigenvector_2, \dots, eigenvector_k$, the data

set $X_{SSP}(t)$ after SSP equals

$$X(t)_{SSP} = \{(0) (0) (0) (0) (0) A_{6,\dots,k}\} A^{-1} X_{raw}(t) \quad (1)$$

where $X_{raw}(t)$ is the raw data set.

2.3 Coherence between MEG and LFP Channels

In order to map frequency-specific coupling between cortical and BG activity, coherence has been applied. Coherence (COH) is a frequency-indexed measure quantifying the extent of two signals holding a consistent phase difference (if a certain frequency is present in both signals) and is defined as follows:

$$COH(f) = \left| \frac{\langle M_n(f) s^*(f) \rangle}{\sqrt{\langle M_n(f) M_n^*(f) \rangle \langle s(f) s^*(f) \rangle}} \right| \quad (2)$$

where $M_n(f)$ is the Fourier transform of a time domain MEG channel and $s(f)$ the Fourier transform of an LFP signal. Coherence has been calculated between all magnetic channels and one LFP electrode contact each before and after SSP (Figure 4 and 3).

3 RESULTS

After CCA removal by SSP, topographic distributions have changed and specifically spread out coherence patterns below 10 Hz are removed (Figure 3). After SSP, coherence between the STN and ipsilateral sensorimotor and premotor areas are found in the beta band (13 to 30 Hz) in most of the PD patients during OFF state, such as the one shown in Figure 3. This feature is less pronounced when PD patients are ON dopaminergic medication. Some of the dystonic patients show a similar coherence pattern between the GPi and cortical areas. Not consistently, but in some of the dystonic patients, coherence between cortical prefrontal areas and the GPi in the alpha frequency band (7 to 12 Hz) becomes apparent after CCA removal (Figure 4).

4 DISCUSSION AND CONCLUSIONS

The SSP approach is based on *a priori* spatial separation of the CCA and cortical brain signals and the topography of the CCA is quite well defined, so this way of artefact removal works adequately for our type of magnetoencephalographic data. Our method is an

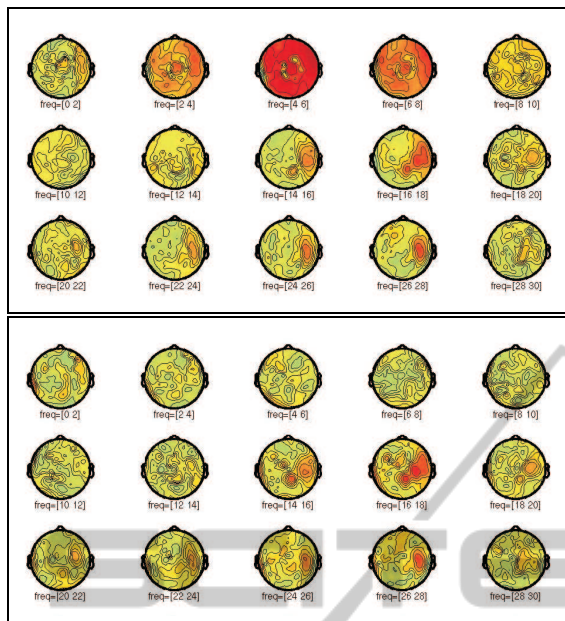


Figure 3: Coherence before (top plot) and after (bottom plot) SSP in a PD patient between all magnetic channels and contact 2 of the right electrode in the STN for frequency bins of 2 Hz size from 0 to 40 Hz.

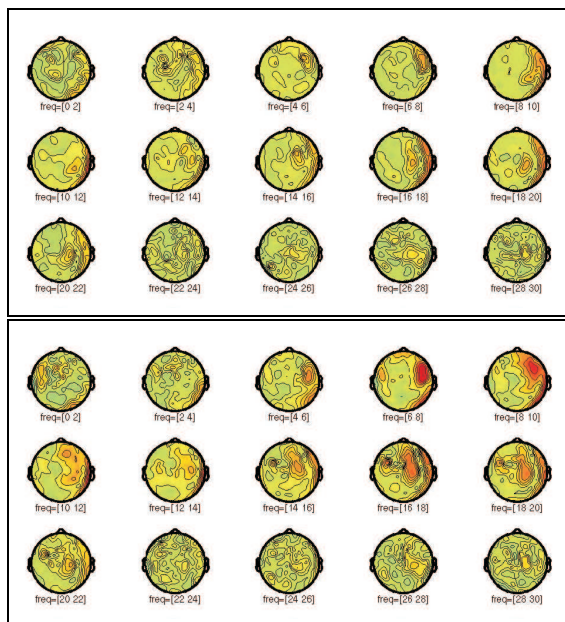


Figure 4: Coherence before (top plot) and after (bottom plot) SSP in a dystonic patient between all magnetic channels and contact 3 of the right electrode in the GPI for frequency bins of 2 Hz size from 0 to 40 Hz.

alternative to optimised beamforming (Litvak et al., 2010) with regard to artefact suppression. In contrast to beamforming, SSP does not require an electrical source model. CCA removal not only suppresses co-

herences that are caused by the CCA, but also uncovers coupling between the basal ganglia and cortical brain regions, which were not visible before SSP. The advantage of beamforming is that the location of the coherent current in the brain is found. PCA on aCCA followed by SSP could therefore be used as a preprocessor for beamforming.

Future work has to investigate the reasons for the CCA influencing coherences and statistical testing of coherence differences before and after SSP (Maris et al., 2007).

ACKNOWLEDGEMENTS

We would like to thank K. Obermayer for helpful discussions and support. A. B. is supported by a fellowship from Dr. Robert Leven und Dr. Maria Leven-Nivelstein-Stiftung.

REFERENCES

- Jousmäki, V. and Hari, R. (1996). Cardiac artifacts in magnetoencephalogram. *Journal of Clinical Neurophysiology*, 13:172–176.
- Kühn, A. A., Williams, A., Kupsch, A., Limousin, P., Hariz, M., Schneider, G. H., Yarrow, K., and Brown, P. (2004). Event-related beta desynchronization in human subthalamic nucleus correlates with motor performance. *Brain*, 127:735–746.
- Litvak, V., Jha, A., Oostenveld, R., Barnes, G. R., Penny, W. D., Zrinzo, L., Hariz, M. I., Limousin, P., Friston, K. J., and Brown, P. (2010). Optimized beamforming for simultaneous MEG and intracranial local field potential recordings in deep brain stimulation patients. *Neuroimage*, 50:1478–1588.
- Maris, E., Schoffelen, J. M., and Fries, P. (2007). Nonparametric statistical testing of coherence differences. *J Neurosci Methods*, 163:161–175.
- Silberstein, P., Kuehn, A. A., Kupsch, A., Trottenberg, T., Krauss, J. K., Woehrle, J. C., Mazzone, P., Insola, A., Lazzaro, V. D., Oliviero, A., Aziz, T., and Brown, P. (2003). Patterning of globus pallidus local field potentials differs between Parkinson’s disease and dystonia. *Brain*, 126:2597–2608.
- Uusitalo, M. A. and Ilmoniemi, R. J. (1997). Signal-space projection method for separating MEG or EEG into components. *Medical and Biological Engineering and Computing*, 35:135–140.